

Environmental Science and Pollution Research

Pyrolysis temperature influences the capacity of biochar to immobilize copper and arsenic in mining soil remediation

--Manuscript Draft--

Manuscript Number:	ESPR-D-22-12629	
Full Title:	Pyrolysis temperature influences the capacity of biochar to immobilize copper and arsenic in mining soil remediation	
Article Type:	Research Article	
Keywords:	Biochar, soil remediation, copper, arsenic, Nature-Based Solutions.	
Corresponding Author:	Ruben Forján Castro, PhD University of Oviedo: Universidad de Oviedo Vigo, Pontevedra SPAIN	
Corresponding Author Secondary Information:		
Corresponding Author's Institution:	University of Oviedo: Universidad de Oviedo	
Corresponding Author's Secondary Institution:		
First Author:	Sandra Rúa Díaz	
First Author Secondary Information:		
Order of Authors:	Sandra Rúa Díaz	
	Ruben Forján Castro, PhD	
	Manoel Lago Vila	
	Beatriz Cerqueira Cancelo	
	Elena Arco Lázaro	
	Purificación Marcet	
	Diego Baragaño	
	José Luis Rodríguez Gallego	
	Emma Fernández Covelo	
Order of Authors Secondary Information:		
Funding Information:	Ministerio de Economía y Competitividad (MCI-20-PID2019-106939GB-I00)	Full Professor José Luis Rodríguez Gallego
	Ministerio de Ciencia, Innovación y Universidades (MU-21-UP2021-030 32892642)	PhD Diego Baragaño
	Consellería de Cultura, Educación e Ordenación Universitaria, Xunta de Galicia (ED481B-2018/075)	PhD Beatriz Cerqueira Cancelo
Abstract:	<p>Biochar is a promising material used for multiple remediation approaches, mainly in polluted soils. Its properties can differ depending on feedstock and pyrolysis temperature. In this context, we tested the capacity of three biochar products made from corncob, pyrolyzed at different temperatures (350, 500, and 650 °C), to remediate a mining soil affected by high levels of Cu and As. We performed an exhaustive characterization of the biochar. We found that biochar showed a higher surface area with increasing pyrolysis temperature, whereas high molecular weight PAHs were detected in biochar produced at the maximum temperature, thus indicating potential ecotoxicological risks. After the application of biochar to the soil, Cu was partially immobilized, especially when using that obtained at 500 °C. This effect is attributed to</p>	

	<p>the structure of this material and an increase in soil pH and organic matter content. Conversely, As was increased in the soluble fraction for all three types of biochar but in a proportion that lacks relevance. On the whole, given its lower PAH content, higher Cu immobilization ratio, and an almost negligible increase in As availability, biochar obtained at 500 °C outperformed the other two products with respect to soil recovery. Of note, data on Cu and As availability were doubled-checked using two extraction methodologies. We propose that this operational approach for determining the most suitable pyrolysis temperature will find application in other soil remediation actions</p>
Suggested Reviewers:	<p>Daniel Arenas Lago University of Vigo - Lagoas Marcosende Campus: Universidade de Vigo darenas@uvigo.es</p> <p>Erika S. Santos Universidade de Lisboa erikasantos@isa.ulisboa.pt</p> <p>Manhattan Lebrun Orleans University: Universite d'Orleans manhattan.lebrun@univ-orleans.fr</p>
Opposed Reviewers:	
Additional Information:	
Question	Response
§Are you submitting to a Special Issue?	No

1 **Pyrolysis temperature influences the capacity of biochar to immobilize**
2 **copper and arsenic in mining soil remediation**

3 Sandra Rúa-Díaz¹, Rubén Forjan^{4*}, Manoel Lago-Vila¹, Beatriz Cerqueira¹, Elena Arco-Lázaro²,
4 Purificación Marcet³, Diego Baragaño⁴, José Luis R. Gallego⁴, Emma F. Covelo¹

5 ¹ Departamento de Biología Vegetal y Ciencia del Suelo, Facultad de Biología, Universidad de
6 Vigo, Vigo, España.

7 ² Departamento de Producción Vegetal en Zonas Tropicales y Subtropicales, Instituto Canario de
8 Investigaciones Agrarias, Santa Lucía de Tirajana, España.

9 ³ Departamento de Biología Vegetal y Ciencia del Suelo, Escuela de Forestales, Universidad de
10 Vigo, Vigo, España.

11 ⁴ INDUROT and Environmental Biogeochemistry & Raw Materials Group, Campus of Mieres,
12 University of Oviedo, 33600 Mieres, Spain.

13 *Corresponding author: rforjan@uvigo.es

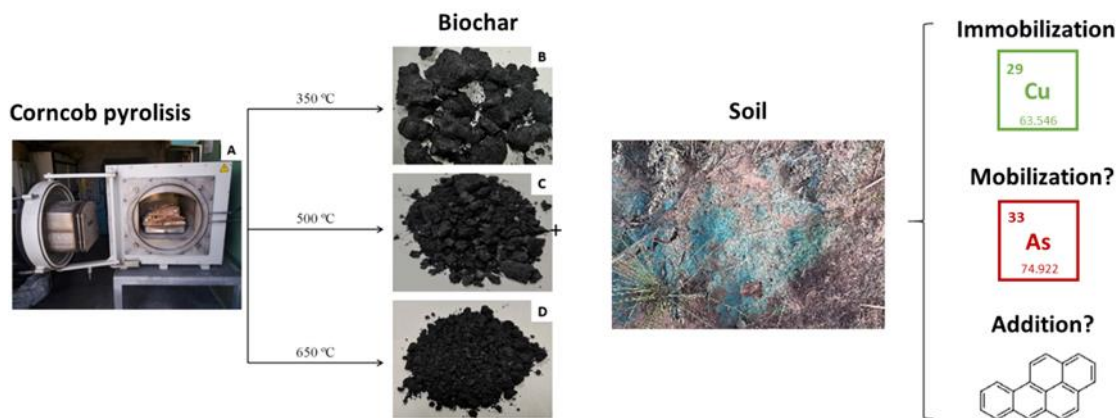
14 **Abstract**

15 Biochar is a promising material used for multiple remediation approaches, mainly in polluted
16 soils. Its properties can differ depending on feedstock and pyrolysis temperature. In this context,
17 we tested the capacity of three biochar products made from corncob, pyrolyzed at different
18 temperatures (350, 500, and 650 °C), to remediate a mining soil affected by high levels of Cu and
19 As. We performed an exhaustive characterization of the biochar. We found that biochar showed
20 a higher surface area with increasing pyrolysis temperature, whereas high molecular weight PAHs
21 were detected in biochar produced at the maximum temperature, thus indicating potential
22 ecotoxicological risks. After the application of biochar to the soil, Cu was partially immobilized,
23 especially when using that obtained at 500 °C. This effect is attributed to the structure of this
24 material and an increase in soil pH and organic matter content. Conversely, As was increased in
25 the soluble fraction for all three types of biochar but in a proportion that lacks relevance. On the
26 whole, given its lower PAH content, higher Cu immobilization ratio, and an almost negligible
27 increase in As availability, biochar obtained at 500 °C outperformed the other two products with
28 respect to soil recovery. Of note, data on Cu and As availability were doubled-checked using two
29 extraction methodologies. We propose that this operational approach for determining the most
30 suitable pyrolysis temperature will find application in other soil remediation actions.

31 **Key words:** Biochar, soil remediation, copper, arsenic, Nature-Based Solutions.

32

33 Graphical abstract



34

35

36

37 1. Introduction

38 One of the main environmental impacts of mining activity is contamination by potentially toxic
39 elements (PTEs) (Akala and Lal, 2000; Shrestha and Lal, 2011; Li et al. 2014). PTEs can promote
40 physical-chemical alterations of mining soils and such changes can extend into areas far from the
41 mine (Ghosh and Maiti 2020). In this context, mining areas affected by pollution usually present
42 a low content of organic matter (OM) and nutrients, decompensated cation exchange capacity
43 (CEC), low water retention capacity, high electrical conductivity, altered pH, little or no
44 vegetation cover, and high available concentrations of PTEs. Such characteristics impair soil
45 ecosystem services (Ussiri and Lal, 2005; Zhou et al. 2015; Pietrzykowski 2019). Open-pit mining
46 in particular causes loss of basic pedological properties. In this context, poor management of
47 settling ponds and tailings can be a major environmental issue. In fact, mine tailings are
48 susceptible to alteration by erosion, leading to increased mobility and leaching of PTEs (Forján
49 et al. 2019), which become a continuous source of long-term contamination until they are
50 stabilized by natural processes. This contamination affects environmental compartments (mainly
51 soil, surface water, and groundwater) close to mine tailings, as well as wider areas, which can
52 lead PTEs to enter the food chain (Mombo et al. 2015; Puga et al. 2016). In this context, and given
53 that the mobility, toxicity, and bioavailability of PTEs do not depend solely on their

54 concentrations, the examination of chemical speciation is critical to understand contamination by
55 these toxic compounds (Gamboa-Herrera et al. 2021).

56 Reclamation strategies are required to reduce the incidence of PTE movement into adjacent
57 ecosystems via water and air erosion (Trippe et al. 2021). Soil recovery is currently being
58 promoted through the provision of Nature-Based Solutions (NBS), which are defined as strategies
59 inspired and supported by nature that are cost-effective and simultaneously provide
60 environmental, social, and economic benefits (European Commission, 2017). NBS offer great
61 potential in the field of contaminated soil remediation, including the application of amendments
62 made from by-products such as biochar, a well-known amendment that effectively improves soil
63 characteristics (Yadav and Garg 2011; Wu et al. 2017; Ghosh and Maiti 2020).

64 Biochar is an amorphous carbonaceous black mass produced by the pyrolytic conversion of
65 organic biomass-a process that yields a porous, low density, carbon-rich material with a large
66 specific surface area (Dowiejuah et al. 2020; Ghosh and Maiti 2020). Biochar has numerous
67 beneficial effects on soil. In this regard, it has been reported to raise soil pH, enhance the OM
68 content and CEC, increase moisture-holding capacity, attract more beneficial fungi and microbes,
69 retain nutrients, and increase carbon sequestration (Beesley et al. 2011; Diacono and Montemurro
70 2011; Beesley et al. 2014; Forján et al. 2017). Of note, biochar can also reduce the availability of
71 PTEs through metal ion complexation on its surface (Beesley et al. 2010; Beesley and Marmiroli
72 2011; Beesley et al. 2011; Park et al. 2011). This complexation capacity is explained by the
73 organic functional groups present on the surface of biochar, such as $-\text{COOH}$, $-\text{CO}-$, $-\text{OH}$, and
74 $\text{R}-\text{COO}-\text{R}$ groups, which have a high capacity to take up metal(loid)s from soil (Ahmad et al.
75 2014, Fellet et al. 2014; Puga et al. 2015; Lomaglio et al. 2017). These effects can be attributed
76 to electrostatic interactions between the negatively charged carbon surface and metal cations, to
77 ionic exchange between metal cations and ionizable protons at the acidic carbon surface, and to
78 sorptive interaction involving delocalized carbon electrons (Sohi et al. 2010). Biochar is more
79 environmentally friendly than active carbon ($-0.9 \text{ kg CO}_2\text{-eq kg}^{-1}$ vs. $6.6 \text{ kg CO}_2\text{-eq kg}^{-1}$) and
80 production costs are lower. In this regard, production costs for granular activated carbon and
81 powdered activated carbon were estimated at \$6.40 and \$1.20-2.00 per kg^{-1} , respectively, whereas

82 several types of biochar were reported to have an average price of \$0.90 per kg⁻¹ (Alhashimi and
83 Aktas 2017; Sizirici et al. 2021).

84 The behaviour of biochar can differ depending on the anionic or cationic nature of PTEs (Beesley
85 et al. 2011; Park et al. 2011; Manyà 2012; Fellet et al. 2014; Luo et al. 2014; Baragaño et al.
86 2020). Furthermore, the interaction of biochar with PTEs may also vary in function of its chemical
87 and physical properties (Duwiejuah et al. 2020; Głąb et al. 2021), which are related to the
88 pyrolysis temperature and source material used for its production (Kloss et al. 2012; Chen et al.
89 2016). The effects of fine-tuning pyrolysis temperature may imply a loss of acidic functional
90 groups and an increase in the amount of ash, as well as variations in the concentration of exchange
91 cations on the surface area, density, and pore diameter (Antal and Grønli 2003; Lin et al. 2008;
92 Budai et al. 2014; Ippolito et al. 2015). In addition, the potential presence of polycyclic aromatic
93 hydrocarbons (PAHs) (Singh et al. 2010; Hale et al. 2012) may also be affected by pyrolysis
94 temperature. Therefore, there is currently controversy regarding the application of biochar to all
95 soil types as some kinds might supply PAHs to this matrix (Xing et al. 2021).

96 Raw biomass for biochar production usually comes from organic waste, thereby promoting the
97 circular economy (agroforestry biomass, livestock waste, urban or industrial waste, etc.) (Beesley
98 et al. 2011). A good example of such a waste product is corncobs, which are generated in high
99 numbers because maize is one of the most common staple crops worldwide (Szufa et al. 2020).
100 Biochar made from maize waste can remove a large number of contaminants from soil (Lehmann
101 and Joseph 2015; Sizirici et al. 2021).

102 Given the above considerations, here we comprehensively evaluated the properties of corncob
103 biochar produced at three temperatures and the behaviour of these materials when used to amend
104 mining soil containing metal(loid)s. In particular, we addressed the interaction of the biochar with
105 Copper (Cu, metal) and Arsenic (As, metalloid), both abundant in the mining soil under study.

106

107 **2. Material and methods**

108 **2.1. Soil sampling**

109 Soil affected by As and Cu pollution was sampled in an area close to a metal mine in NW Spain
110 that has been active for decades. Several soil subsamples were taken at a depth of 30 cm. These
111 were then mixed and a 50-kg composite sample was obtained. The composite sample was taken
112 to the laboratory, air-dried, sieved through 2-mm mesh, and homogenized.

113

114 **2.2. Soil analyses**

115 The pseudo-total concentrations of As and Cu were determined after extraction with aqua regia
116 1:3 (v/v) (HNO₃ / HCl) in a microwave oven (Milestone ETHOS 1) and analysis by ICP-OES
117 (Perkin-Elmer; Optima 4300 DV). Soil texture data were obtained following Guitián and
118 Carballas (1976) and USDA criteria to determine soil texture (USDA 1982). Clays were
119 qualitatively identified following the procedure described by Brown and Brindley (1980) using
120 X-ray diffraction (XRD) analysis. A powder X-ray diffraction (PXRD) pattern was obtained using
121 a SIEMENS D-5000 diffractometer (with a Cu K α 1 radiation source). pH was measured with an
122 electrode in a 1:2.5 ratio of water to sample following the method described by Guitián and
123 Carballas (1976). Total carbon (TC) and total nitrogen (TN) were measured in the solid sample
124 module of a LECO elemental macro-analyzer (CNS2000), while a bidistilled water extraction
125 was carried out to measure dissolved organic carbon (DOC), following Sanchez-Monedero et al.
126 (1996). The Mehlich III method (Mehlich 1984) was used to determine available phosphorus
127 (AP). Organic matter (OM) was measured by weight loss on ignition (LOI: loss on ignition)
128 (Beaudoin 2003). Exchangeable cations (Ca²⁺, K⁺, Mg²⁺, Na⁺, and Al³⁺) were extracted with 0.1M
129 BaCl₂ (Hendershot and Duquette 1986) and their concentrations were determined by ICP-OES
130 (Perkin-Elmer; Optima 4300 DV). Cation exchange capacity (CEC) was calculated by adding the
131 total concentrations of exchangeable cations. The concentrations of free oxides of Fe, Al and Mn
132 were determined using the method described by Mehra and Jackson (1960), with subsequent
133 measurement by ICP-OES (Perkin-Elmer; Optima 4300 DV).

134

135 **2.3. Biochar production and characterization**

136 Three types of biochar were produced using corncobs as raw biomass. The biochar was developed
137 in collaboration with the company Centro de Valorización Ambiental del Norte S.L. (Touro, A
138 Coruña). The furnace used (model HCV_56 CCH) was designed by Forns Hobersal SL. Biochar
139 is usually obtained at temperatures above 250 °C irrespective of the source of biomass (Lehmann
140 and Joseph 2015; Sizirici et al. 2021). In our case, the pyrolysis temperatures selected were as
141 follows 350 °C (B350), 500 °C (B500) and 650 °C (B650) (Fig. S1A, S1B, S1C Supplementary
142 Material). The raw material was pre-dried so that the starting conditions were the same for all
143 pyrolytic procedures. After pyrolysis, the biochar was air-dried, ground and sieved to 2 mm to
144 homogenize the biochar particles and to equalize them to the soil fraction which is considered
145 below 2 mm. The general pyrolysis times, temperatures, and yields obtained for each biochar
146 product are shown in Table S1 (Supplementary Material). As expected, the yield was lower with
147 increasing pyrolysis temperature due to a greater loss of biomass. These yield data are consistent
148 with those obtained by Szufa et al. (2020) and Das et al. (2021).

149 The biochars obtained were subjected to the following determinations. First, the specific surface
150 area (SSA) was measured by CO₂ adsorption at 77 K using an ASAP 2020 Micromeritics analyzer
151 on samples previously outgassed at 373 K for 2 h. Complementarily, pore size distribution was
152 determined following the Dubinin-Stoeckli model. CHN concentrations were measured in a
153 LECO CN-2000 module, oxygen content was calculated by difference. Biochar surface was
154 observed using a JEOL JSM-5600 Scanning Electron Microscope. To obtain information about
155 the presence of ash in the biochar, thermogravimetric curves (TGA) and differential scanning
156 calorimetry (DSC) were achieved from ambient temperature to 1273 K at a heating rate of 283 K
157 min⁻¹ in an inert N₂ atmosphere using an SDT Q600 instrument. Finally, to determine PAHs, 5-g
158 representative subsamples were extracted by dichloromethane:acetone (1:1) in a Soxtherm
159 apparatus (Gerhardt), according to a usual protocol (Boente et al. 2020). The 16 priority PAHs
160 were measured after injection into a 7890A GC System coupled to a 5975C Inert XL MSD with
161 a Triple-Axis Detector (Agilent Technologies) and following a modification of EPA method
162 8272. A capillary column DB-5 ms (5% phenyl and 95% dimethylpolysiloxane) 30 m × 0.25 mm
163 i.d. × 0.25 µm film (Agilent Technologies) was used, with He as carrier gas at a flow rate of 1 mL

164 min⁻¹. The initial oven temperature was 80 °C (held for 2 min), which was ramped up at 15 °C/min
165 to 300 °C (held for 10 min). The GC injector was operated in splitless mode for 2 min at 260 °C.
166 The mass spectrometer was operated in selected ion monitoring mode (SIM), and the m/z ratios
167 for PAHs quantification were 128, 152, 153, 154, 165, 166, 178, 202, 228, 252, 276, and 278I.
168 Calibration mixtures (AccuStandard) were used.

169

170 **2.4. Experimental design and pollutant mobility**

171 The soil (S) was subjected to the following four treatments:

- 172 - S: Initial mining soil.
- 173 - SB350: S + corncobs pyrolyzed at 350 °C (B350).
- 174 - SB500: S + corncobs pyrolyzed at 500 °C (B500).
- 175 - SB650: S + corncobs pyrolyzed at 650 °C (B650).

176 The samples (100-g, dry weight) with a soil:biochar ratio of 95:5 (w/w) were incubated in 500-
177 mg glass jars in triplicate for 40 days under controlled conditions of darkness, temperature (22 ±
178 2 °C) and water content (maintained around field capacity by adding distilled water periodically).
179 At the end of the experiments, samples were air-dried, passed through a 2-mm sieve, and
180 homogenized prior to analysis. To monitor the available concentrations of As and Cu, these metal
181 and metalloid were extracted with 0.01 M CaCl₂ in soil solution (Houba et al. 2000) and their
182 concentrations were determined by ICP-OES (Perkin-Elmer; Optima 4300 DV).

183 Furthermore, and to gain a deeper understanding of pollutant mobility, a sequential extraction
184 was carried out following the procedure described by Salbu et al. (1998), modified from the
185 method of Tessier et al. (1979). The concentrations of As and Cu were fractionated into mobile
186 phases (F1: Water-soluble, F2: Exchangeable, and F3: Bound to carbonates) and less mobile or
187 immobile phases (F4: Bound to iron and manganese oxides, F5: Bound to organic matter, and F6:
188 Residual) by means of extractants of increasing strength from fraction 1 to fraction 6.

189 After each extraction, the samples were centrifuged, and the extracts were clean with syringes
190 with 0.45-µm filters (Sartorius Minisart) into 50-ml glass tubes (using the same syringe and filter

191 for each of the replicates during the entire process). Each sample residue was washed with 10 ml
192 of bidistilled water (water was added, stirred manually, and centrifuged for another 15 min at
193 3300 rpm), and the resulting extract was added to the extract obtained in that fraction. The extracts
194 obtained were analyzed by ICP-OES (Perkin-Elmer; Optima 4300 DV).

195

196 **2.5. Statistical analysis**

197 All analytical determinations were performed in triplicate. The data obtained were processed
198 statistically using the SPSS program for Windows (version 24.0), taking statistical significance
199 with p values <0.05. Normality tests (Kolmogorov-Smirnov test), Levene's homogeneity of
200 variances, and analysis of variances (ANOVA) were performed. In the case of homogeneity of
201 variances, a post hoc least significant distance (LSD) test was performed, while if there was no
202 homogeneity of variances, Dunnett's T3 test was carried out. In addition, a Pearson's bivariate
203 correlation analysis was also performed.

204

205 **3. Results and discussion**

206 **3.1. General characteristics of the biochar and mining soil**

207 Pseudo-total concentrations of As and Cu in the initial soil were higher than in natural soils,
208 whereas the contents of these PTEs in the three biochar products were almost negligible.
209 Concretely, As concentrations in the three pyrolyzed biochar products remained below the
210 quantification limit (0.001 mg L⁻¹), while soil content was 85.09 mg kg⁻¹. At the same time, Cu
211 concentration in soil was 1124 mg kg⁻¹, while in the biochar products it was below 10 mg kg⁻¹,
212 with slightly increasing values as the pyrolysis temperature increased (Table 1). The chosen soil
213 belongs to a mine tailing, according to the USDA (1982), the initial soil can be classified as loam-
214 sandy-clay. The XRD analysis indicated that the clay fraction consisted mainly of kaolinite,
215 montmorillonite and illite (Fig. S2, Supplementary Material), while other silicates such as quartz
216 were also present (Table S2, Supplementary Material).

217 Oxide analysis of the initial soil showed high concentrations of Fe oxides and considerable
218 concentrations of Al oxides, while concentrations of Mn oxides were low (Table 1). The initial

219 soil had an acidic pH while three biochar products were alkaline. Biochar pH values (B350, B500
220 and B650) increased with pyrolysis temperature, as previously indicated by Duwiejuah et al.
221 (2020). The soil had a lower OM and TC content than the biochar, whereas the increase in
222 pyrolysis temperature caused a slightly decrease in the OM content of the latter, whereas the
223 higher the pyrolysis temperature, the higher the TC content. This result might be due to the yield
224 being lower at 650 °C and are consistent with those reported by Kim et al. (2021) and Das et al.
225 (2021), who concluded that biochar TC content increases up to 10.14% with pyrolysis
226 temperature. In turn, we observed that the biochar products had a higher DOC content than the
227 soil (Table 1) and that biochar pyrolyzed at higher temperature had a greater DOC content than
228 that produced at 350°C. These data contrast with those obtained by authors such as Luo et al.
229 (2015) and Uchimiya et al. (2013), who concluded that an increase in pyrolysis temperature leads
230 to a decrease in DOC content. The biochar products showed a higher TN content and available P
231 concentration than soil (Table 1). In this regard, B350 had a higher available P concentration than
232 B500 and B650, whereas TN was almost the same. These results are in line with the conclusions
233 obtained by Mukherjee and Zimmerman (2013). All three biochar products had a higher CEC
234 than the initial soil (Table 1) and, specifically, B500 and B650 had a higher CEC than B350.
235 Remarkably, the high CEC values of the products were due mainly to their high concentrations
236 of K⁺. It should also be noted that Al³⁺ was undetectable in these amendments, and thus the base
237 saturation values (V) were 100% in all three cases; however, the Al³⁺ concentration in soil was
238 11.60 cmol₍₊₎kg⁻¹.

239

240 **3.2. Specific biochar characterization**

241 The specific surface area (SSA) of the biochar products increased progressively with pyrolysis
242 temperature (Table 1), in agreement with Zhang et al. (2011), who deduced an increase in
243 aromatic C content and the progressive destruction of –OH groups, ester C=O bonds, aliphatic -
244 CH₂, and C–O groups shielding the aromatic core as the pyrolytic temperature rises, i.e., the
245 increase in aromatic C content enlarges the SA. Furthermore, this higher SSA is possibly due to
246 a decrease in pore size as pyrolysis temperature rises (Sizirici et al. 2021). In this regard, the

247 largest difference in pore size was found between B350 and the other two amendments (B500 and
248 B650) (Fig. S3, Supplementary Material); these differences also coincide with differences in SSA.
249 In addition, it is possible to observe this using SEM, as it is revealed in Fig. S1 (Supplementary
250 Material). C/H and C/O ratios indicate degree of aromaticity and polarity, respectively, which are
251 critical properties to evaluate the carbon structure of this material (Xing et al., 2021). The molar
252 H/C ratio is important as it gives an indication of the degree of carbonization of biochar (Das et
253 al., 2021; Mohan et al., 2018). In our case, contrary to what might be expected, B350 and B650
254 showed identical degrees of carbonization (Table 1). In turn, authors such as Mohan et al. (2018)
255 and Das et al. (2021) took the C/O molar ratio as an indicator of the hydrophilicity of the biochar
256 surface because it reflects the content of polar groups derived mainly from carbohydrates. We
257 found that the value of the C/O ratio followed the sequence B500 > B650 > B350 (Table 1),
258 thereby suggesting that biochar produced at 500 °C is the most hydrophilic.

259 The thermogravimetric analysis (TGA) curve (Fig. S3, Supplementary Material) of the three
260 biochar products revealed that B350 lost more mass (weight %) and more rapidly than B500 and
261 B650. Higher losses at lower temperatures could be explained by moisture as the mass loss from
262 0 °C to 250 °C was due to the release of water (volatilization), together with the formation and
263 release of volatile gaseous products such as CO, CO₂, CH₃COOH, and other organic compounds
264 (Szufa et al., 2020; Das et al., 2021). The mass loss from 250 °C to 600 °C was caused by thermal
265 decomposition of the biomass and decomposition of lignocellulosic substances (Cao and Harris
266 2010; Das et al. 2021). In this regard, corncob has three main components, namely hemicellulose,
267 cellulose, and lignin, and these compounds pyrolyze at different temperatures and thus influence
268 the TGA curve of each biochar product (Ouyang et al. 2015). The mass loss from 600 °C and
269 above could be attributable to, among other factors, the decomposition of calcium phosphate and
270 inorganic minerals such as calcite (CaCO₃) (Das et al. 2021). Regarding the PAH content of each
271 biochar product, quantitative data are shown in Table 2. In our case, biochar pyrolyzed at the
272 lowest temperature had a higher content of low molecular weight PAHs (2-3 aromatic rings),
273 whereas the highest temperature promoted an abundance of heavy molecular weight PAHs (4 or
274 more aromatic rings). Of note, the total concentration of PAHs was the lowest at the intermediate

275 temperature (500 °C) and thus this material emerges as the best option as a soil amendment in
276 terms of reducing potential toxicity.

277 **3.3. Biochar treatments of polluted soil.**

278 **3.3.1. pH, organic matter, and dissolve organic carbon evolution.**

279 The three treatments applied caused a moderate but significant ($p < 0.05$) increase in soil pH (Fig.
280 1A). However, in all cases, the soil treated with biochar continued to maintain an acidic pH. The
281 increase in pH observed is consistent with previous work on biochar treatment of mining soils
282 (Zhao et al. 2015; Rodríguez-Vila et al. 2017). This increase is probably caused mainly by the
283 association of H^+ ions with the biochar and subsequent decarboxylation processes (Solaiman et
284 al. 2015). The SB500 treatment led to the greatest increase in pH (Fig. 1A), possibly because this
285 amendment had a greater CEC due to its higher content of the basic cation K^+ (Table 1). In this
286 regard, high CEC and %K are often correlated with high pH values (Canet et al. 2007; Alvarenga
287 et al. 2008; Forján et al. 2018). The increase in pH after soil treatment with biochar was lower
288 than expected, possibly due to a low buffering capacity of the soil, a common effect in acidic soil
289 such as that found in and around mines (Baileys and Blankenhord 1982, Beesley et al. 2014,
290 Budai et al. 2014, Forján et al. 2018). Regarding potential acidity (pH_{KCl}), in the control soil, this
291 parameter was less than 3.4, and a significant increase ($p < 0.05$) was observed after the addition
292 of biochar, reaching a maximum of 4.3 in SB500. On the whole, an increase in pH, although
293 restrained in our case, may influence other soil properties and thereby mobilize metalloids
294 (Ahmad et al. 2014; Duwiejuah et al. 2020).

295 The addition of B350, B500, and B650 to the mining soil caused an increase in OM content. This
296 increase was more notable with biochar produced at higher pyrolysis temperatures (Fig. 1B),
297 conversely to what could be expected since, for instance, B350 had a higher OM content than
298 B650. Therefore, and also taking into account (Fatima et al. 2021) that the amendment of soil
299 with biochar can reduce the decomposition of soil OM, we conclude that the increase in pyrolysis
300 temperature improves the capacity of biochar to retain organic matter by mechanisms such as
301 adsorption (Duwiejuah et al. 2020, Xing et al. 2021). In turn, the increase in OM caused a

302 significant increase in DOC in all treatments (Fig. 1C), i.e., a remarkable positive correlation was
303 observed between OM and DOC ($0.94, p < 0.01$). A greater increase in DOC content was expected
304 in the SB500 and SB650 treatments since the biochar prepared at 500 °C and 650 °C had a much
305 higher initial DOC content than B350 (Table 1). However, the greatest increase in soil DOC was
306 induced by B350, which is in agreement with Li et al. (2018), who observed that biochar
307 pyrolyzed at low temperatures leads to a greater increase in this parameter than that produced at
308 higher temperatures.

309 3.3.2. Evaluation of Cu sequential extraction

310 The chemical distribution of Cu is shown in Fig. 2. On the whole, and irrespective of the
311 treatment, a similar concentration of immobile Cu (F4 to F6) and mobile Cu (F1 to F3) was found.
312 This behaviour was not observed in the control soil, in which there was a higher concentration of
313 Cu in the mobile than in the immobile phase. This trend was more evident in the case of the SB500
314 treatment, especially for F1. In the most mobile phases (F1 and F2), the availability of Cu
315 decreased significantly ($p < 0.05$) in all three biochar treatments (Fig. 2A). The maximum
316 reduction was observed in the SB500 treatment (from 234 mg kg⁻¹ in the control down to 121 mg
317 kg⁻¹ in F1). Similarly, exchangeable Cu in F2 (Fig. 2B) was decreased from 386 mg kg⁻¹ in the
318 control down to 302 mg kg⁻¹ in SB500. On the contrary, in the fraction bound to carbonates (F3,
319 Fig. 2C), the concentration of Cu was increased, being more significant in treatments SB500 and
320 SB650. Regarding the less mobile fractions, F4 and F5 (Fig. 2D and Fig. 2E), there were only
321 slightly significant differences in F5 between the control and the treatments. Finally, the residual
322 fraction, F6, remained essentially stable irrespective of the biochar used.

323 As indicated by these results, the most bioavailable fractions (F1 and F2) tended to show
324 immobilization, especially in the SB350 and SB500 treatments. This observation is consistent
325 with the findings of Solaiman et al. (2015) as the two most important factors affecting the
326 bioavailability of toxic metals are the OM content and pH of the soil. In our case, the increase in
327 pH described is expected to have promoted the precipitation of Cu carbonates. In the same sense,
328 negative correlations were found between OM vs. pH and Cu concentrations in F1 and F2, with

329 values of -0.91, -0.95 ($p < 0.01$) and -0.78, -0.80 ($p < 0.01$), respectively. Several authors obtained
330 similar results (a decrease in Cu availability) when pH and OM values were increased (Park et al.
331 2011; Pérez-Esteban et al. 2012; Forján et al. 2016). Also, and according to Sizerici et al. (2021),
332 Cu removal efficiency and sorption capacity increase more in a pH range from 2 to 6 while at
333 higher pH the growth in sorption efficiency is lower. In our case, SB500 caused the greatest
334 increase in pH (from 3.42 to 4.27), becoming the treatment with the highest Cu sorption efficiency
335 in these first two fractions. Complementarily to pH effects, the decrease in Cu concentrations in
336 the most mobile phases (F1 and F2) was significantly negatively correlated with the DOC
337 provided by the treatments (-0.92 and -0.91, $p < 0.01$), thus Cu can also be complexed by DOC
338 and subsequently its concentration decreases (Beesley et al. 2014).

339 The reduction of Cu bioavailability can be explained not only by the chemical effects of biochar
340 amendments but also by the intrinsic properties of the different biochar material used. In this
341 regard, B500 and B650 had higher SSAs and smaller and more homogeneous pores than B350,
342 and these two factors should improve Cu immobilization (Chen et al. 2014; Sizerici et al. 2021).
343 In fact, the functional groups present on the biochar surface confer adsorption potential for toxic
344 compounds such as Cu (Uchimiya et al. 2010; Duwiejuah et al. 2020). In addition, the increase in
345 SA also increases the number of functional groups that interact with pollutants.

346 **3.3.3. Evaluation of As sequential extraction**

347 The results are shown in Fig. 3. Note that only F1, F4, F5, and F6 are shown as F2 and F3 values
348 were below the quantification limit. The initial As availability was very low (F1 close to detection
349 limit, Fig. 3A), whereas the most abundant fractions were F4 and F6 (Fig. 3B and Fig. 3D,
350 respectively). A general effect of biochar amendment was slight mobilization (F1 increase but
351 only up to very low concentrations) for all treatments (Fig. 3A), and this was simultaneous to a
352 slight decrease in As in the residual fraction (F6 reduction, Fig. 3D). Although the pH increased
353 significantly in all treatments, it continued to be acidic, as shown in Fig. 1A, and thus positive
354 charges predominated on the soil adsorption surface, allowing As to remain strongly retained (Lin
355 et al. 2008; Hartley et al. 2009; Tack et al. 2010). Therefore, the increase in pH in the SB350,

356 SB500 and SB650 treatments was not enough for relevant mobilization of As. On the contrary,
357 the presence of biochar may favour a slight increase in available As, as the negatively charged
358 functional groups present in biochar repel As anions (Arco-Lázaro et al. 2016; Abou et al. 2019).
359 In the same context, an increase in DOC mobilizes available As (Beesley et al. 2010; Guisquiani
360 et al. 1998; Hartley et al. 2010), given that OM is adsorbed preferentially on the soil aggregates
361 instead of As and/or it forms soluble organometallic complexes with As. However, in this
362 experiment, no correlations were obtained between DOC and F1, perhaps because As
363 concentrations were very low. In turn, as shown previously in Table 1, the biochar products
364 showed a significantly higher P content than the initial soil. This might also partially explain the
365 release of some As to the most mobile fraction due to the competitive interaction between As and
366 P for sorption sites given that P can displace and mobilize As (Hartley et al. 2009; Bolan et al.
367 2013; Fleming et al. 2013; Baragaño et al. 2020). This process occurs most significantly in low
368 pH soils (Xu et al. 2014; Solaiman and Anawar 2015), as occurs in our case (Table 1).

369 **3.3.4. Evaluation of Cu and As availability in CaCl₂ extraction.**

370 To corroborate previous results of sequential extraction and to address potential effects on
371 vegetation, an additional extraction with CaCl₂ was performed. The treatments applied caused a
372 decrease in available Cu, with SB500 being the most effective (Fig. 4A). This decrease is probably
373 due to the increase in pH and OM, as explained above (Weng et al., 2001; Park et al., 2011). In
374 addition, this relationship between pH and OM with available Cu was reflected by negative
375 Pearson correlations, with values of $r=-0.82$, $r=-0.97$ for pH and OM, respectively ($p<0.01$).
376 Again, there was a significantly negative correlation between available Cu and DOC (-0.87 ,
377 $P<0.01$)—an observation that reinforces the results obtained in the previous section. As regards
378 available As, this was below the quantification limit in the initial soil whereas As availability in
379 CaCl₂ increased marginally once the treatments were applied (Fig. 4B), without significant
380 differences between the three biochar products. This behaviour is fully concordant with that of
381 the most mobile fraction of the Tessier extraction described in the previous section.

382 **4. Conclusion**

383 The results reported herein indicate that the use of biochar as an amendment led to an
384 improvement in the physical-chemical characteristics of the mining soil, such as an increase in
385 OM content and pH in all cases, irrespective of the pyrolysis temperature used to prepare the
386 biochar. However, biochar produced at higher pyrolysis temperatures (350 °C > 500 °C > 650°C)
387 showed a higher specific surface area, which is related to Cu immobilization. The SB500 and
388 SB650 treatments were more effective at immobilizing Cu than SB300. Of note, B500 emerges
389 as the amendment of choice as it showed lower concentrations of PAHs and less energy was
390 required for its production. All the biochar treatments led to a slight mobilization of As. However,
391 the very low As availability observed, these changes are not significant enough to cause a relevant
392 effect. The different behaviour of Cu and As in response to biochar amendment were concordant
393 in a sequential extraction procedure and a CaCl₂ extraction, thereby demonstrating the feasibility
394 of using biochar to immobilize metals without remobilizing metalloids. In addition, pyrolysis
395 temperature emerges as a critical parameter to take into account when preparing biochar for
396 remediation purposes.

397 **Author contribution** Sandra Rúa-Díaz: Conceptualization, Investigation, Formal analysis,
398 Writing. Manoel Lago-Vila: Investigation. Beatriz Cerqueira: Investigation, Supervision. Elena
399 Arco-Lázaro: Conceptualization, Investigation. Purificación Marcet: Supervision, Funding
400 acquisition. Rubén Forjan: Investigation, Formal analysis, Writing. Diego Baragaño:
401 Investigation, Formal analysis, Writing. José Luis R. Gallego: Supervision, Project
402 administration, Funding acquisition. Emma F. Covelo: Conceptualization, Supervision, Project
403 administration, Funding acquisition.

404

405 **Funding** This work was partially funded by the Ministerio de Economía y Competitividad
406 (MINECO, Spain) under the project NANOCAREM (AEI/Spain, FEDER/EU, MCI-20-
407 PID2019-106939GB-I00).

408

409 **Data availability** All the experimental data in this paper are obtained through three experiments,
410 and the data are reliable. The materials are derived from daily life and are simple and easy to
411 obtain

412

413 **Declarations**

414 **Ethics approval** This article does not involve human and animal research. The authors of this
415 paper all participated in the research work of the paper. All authors agree to participate in the
416 writing of the paper and agree to publish this article.

417

418 **Consent for publication** Not applicable.

419

420 **Competing interests** The authors declare no competing interests.

421

422 **Acknowledgements** PhD. Beatriz Cerqueira would like to thank the Xunta de Galicia and the
423 University of Vigo for a postdoctoral grant (Ref. ED481B-2018/075). PhD. Diego Baragaño is
424 grateful to the European Union-NextGenerationEU, Ministerio de Universidades, and Plan de
425 Recuperación, Transformación y Resiliencia, through a call of the Universidad de Oviedo, for a
426 postdoctoral grant (Ref. MU-21-UP2021-030 32892642).

427

428 **References**

429 Abou JL, Garau G, Nassif N, Darwish T, Castaldi P (2019) Metal(loid)s immobilization in soils
430 of Lebanon using municipal solid waste compost: microbial and biochemical impact. Appl Soil
431 Ecol 143:134-143. <https://doi.org/10.1016/j.apsoil.2019.06.011>

432 Ahmad M et al (2014) Biochar as a sorbent for contaminant management in soil and water: a
433 review. Chemosphere 99:19-33. <https://doi.org/10.1016/j.chemosphere.2013.10.071>

434 Akala VA, Lal R (2000) Potential of mine land reclamation for soil organic carbon sequestration
435 in Ohio. Land Degrad Dev. 11:289-297. [https://doi.org/10.1002/1099-145X\(200005/06\)11:3<289::AID-LDR385>3.0.CO;2-Y](https://doi.org/10.1002/1099-145X(200005/06)11:3<289::AID-LDR385>3.0.CO;2-Y)

437 Alhashimi HA, Aktas CB (2017) Life cycle environmental and economic performance of biochar
438 compared with activated carbon: a meta-analysis. Resour Conserv Recycl 118:13-26.
439 <https://doi.org/10.1016/j.resconrec.2016.11.016>

- 440 Alvarenga P et al (2008) Evaluation of composts and liming materials in the phytostabilization of
441 a mine soil using perennial ryegrass. *Sci Total Environ* 406:43-56.
442 <https://doi.org/10.1016/j.scitotenv.2008.07.061>
- 443 Antal MJ, Grønli M (2003) The art, science, and technology of charcoal production. *Ind Eng*
444 *Chem Res* 42:1619-1640. <https://doi.org/10.1021/ie0207919>
- 445 Arco-Lázaro E, Agudo I, Clemente R, Bernal MP (2016) Arsenic (V) adsorption-desorption in
446 agricultural and mine soils: effects of organic matter addition and phosphate competition. *Environ*
447 *Pollut* 216:71-79. <https://doi.org/10.1016/j.envpol.2016.05.054>
- 448 Baileys RT, Blankenhorn PR (1982) Calorific and porosity development in carbonized wood.
449 *Wood Sci* 15: 19-28.
- 450 Baragaño D et al (2020) Application of biochar, compost and ZVI nanoparticles for the
451 remediation of As, Cu, Pb and Zn polluted soil. *Environ Sci Pollut Res* 27:33681-33691.
452 <https://doi.org/10.1007/s11356-020-09586-3>
- 453 Beaudoin A (2003) A comparison of two methods for estimating the organic content of sediments.
454 *J Paleolimn* 29:387-390. <https://doi.org/10.1023/B:JOPL.0000013354.67645.d>
- 455 Beesley L, Moreno-Jiménez E, Gomez-Eyles J (2010) Effects of biochar and greenwaste compost
456 amendments on mobility, bioavailability and toxicity of inorganic and organic contaminants in a
457 multi-element polluted soil. *Environ Pollut* 158:2282-2287.
458 <https://doi.org/10.1016/j.envpol.2010.02.003>
- 459 Beesley L, Marmiroli M (2011) The immobilisation and retention of soluble arsenic, cadmium
460 and zinc by biochar. *Environ Pollut* 159:474-480. <https://doi.org/10.1016/j.envpol.2010.10.016>
- 461 Beesley L et al (2011) A review of biochars' potential role in the remediation, revegetation and
462 restoration of contaminated soils. *Environ Pollut* 159 :3269-3282.
463 <https://doi.org/10.1016/j.envpol.2011.07.023>
- 464 Beesley et al (2014) Assessing the influence of compost and biochar amendments on the mobility
465 and toxicity of metals and arsenic in a naturally contaminated mine soil. *Environ Pollut* 186:195-
466 202. <https://doi.org/10.1016/j.envpol.2013.11.026>
- 467 Boente C, Baragaño D, Gallego JR (2020) Benzo[a]pyrene sourcing and abundance in a coal
468 region in transition reveals historical pollution, rendering soil screening levels impractical.
469 *Environ Pollut* 266:115341. <https://doi.org/10.1016/j.envpol.2020.115341>
- 470 Bolan N, Mahimairaja S, Kunhikrishnan A, Choppala G (2013) Phosphorus-arsenic interactions
471 in variable-charge soils in relation to arsenic mobility and bioavailability. *Sci Total Environ* 463:
472 1154-1162. <https://doi.org/10.1016/j.scitotenv.2013.04.016>
- 473 Brown G, Brindley GW (1980) X-ray Diffraction Procedures for Clay Mineral Identification. In:
474 Brindley GW, Brown G. (eds) *Crystal Structures of Clay Minerals and their X-Ray Identification*.
475 Mineralogical Society of Great Britain and Ireland. London, UK. pp 305-360
- 476 Budai A et al (2014) Surface properties and chemical composition of corncob and *Miscanthus*
477 biochars: effects of production temperature and method. *J. Agr. Food Chem.* 62, 3791-3799.
478 <https://doi.org/10.1021/jf501139f>
- 479 Canet R et al (2007) Composting olive mill pomace and other residues from rural southeastern
480 Spain. *Waste Manage* 28:2585-2592. <https://doi.org/10.1016/j.wasman.2007.11.015>

- 481 Cao X, Harris W (2010) Properties of dairy-manure-derived biochar pertinent to its potential use
 482 in remediation. *Bioresour Technol* 101:5222-5228.
 483 <https://doi.org/10.1016/j.biortech.2010.02.052>
- 484 Chen T et al (2014) Influence of pyrolysis temperature on characteristics and heavy metal
 485 adsorptive performance of biochar derived from municipal sewage sludge. *Bioresour Technol*
 486 164:47-54. <https://doi.org/10.1016/j.biortech.2014.04.048>
- 487 Chen XW, Wong JTF, Ng CWW, Wong MH (2016) Feasibility of biochar application on a
 488 landfill final cover: A review on balancing ecology and shallow slope stability. *Environ Sci Pollut.*
 489 *Res* 23:7111-7125. <https://doi.org/10.1007/s11356-015-5520-5>
- 490 Das SK, Ghosh GK, Avasthe RK, Sinha K (2021) Compositional heterogeneity of different
 491 biochar: Effect of pyrolysis temperature and feedstocks. *J Environ Manage* 278:111501.
 492 <https://doi.org/10.1016/j.jenvman.2020.111501>
- 493 Diacono M, Montemurro F (2011) Long-term effects of organic amendments on soil fertility. In:
 494 Lichtfouse E, Hamelin M, Navarrete M, Debaeke P (eds.) *Sustainable Agriculture Volume 2*.
 495 Springer, Dordrecht, Netherlands, pp 761-786 <https://doi.org/10.1051/agro/2009040>
- 496 Duwiejuah AB, Abubakari AH, Quainoo AK, Amadu Y (2020) Review of Biochar Properties and
 497 Remediation of Metal Pollution of Water and Soil. *J Health Pollut* 10:200902.
 498 <https://doi.org/10.5696/2156-9614-10.27.200902>
- 499 European Commission, 2017. Environment-Research & Innovation Policy Topics–Nature Based
 500 Solution.
- 501 Fatima S (2021) Higher biochar rate strongly reduced decomposition of soil organicmatter to
 502 enhance C and N sequestration in nutrient-poor alkaline calcareous soil. *J Soils Sediments* 21:
 503 148-162. <https://doi.org/10.1007/s11368-020-02753-6>
- 504 Fellet G, Marmiroli M, Marchiol L (2014) Elements uptake by metal accumulator species grown
 505 on mine tailings amended with three types of biochar. *Sci Total Environ* 468 :598-608.
 506 <https://doi.org/10.1016/j.scitotenv.2013.08.072>
- 507 Fleming M, Tai Y, Zhuang P, McBride MB (2013) Extractability and bioavailability of Pb and
 508 As in historically contaminated orchard soil: effects of compost amendments. *Environ Pollut* 177:
 509 90-97. <https://doi.org/10.1016/j.envpol.2013.02.013>
- 510 Forján R, Asensio V, Rodríguez-Vila A, Covelo EF (2016) Contributions of a compost-biochar
 511 mixture to the metal sorption capacity of a mine tailing. *Environ Sci Pollut Res* 23:2595-2602.
 512 <https://doi.org/10.1007/s11356-015-5489-0>
- 513 Forján R, Rodríguez-Vila A, Cerqueira B, Covelo EF (2017) Comparison of the effects of
 514 compost versus compost and biochar on the recovery of a mine soil by improving the nutrient
 515 content. *J Geochem Explor* 183:46-57. <https://doi.org/10.1016/j.gexplo.2017.09.013>
- 516 Forján R, Rodríguez- Vila A, Pedrol N, Covelo EF (2018) Application of Compost and Biochar
 517 with Brassica juncea L. to Reduce Phytoavailable Concentrations in a Settling Pond Mine Soil.
 518 *Waste Biomass Valori* 9:821-834. <https://doi.org/10.1007/s12649-017-9843-y>
- 519 Forján R, Rodríguez-Vila A, Covelo EF (2019) Increasing the Nutrient Content in a Mine Soil
 520 Through the Application of Technosol and Biochar and Grown with Brassica juncea L. *Wate*
 521 *Biomass Valori* 10:103–119. <https://doi.org/10.1007/s12649-017-0027-6>

- 522 Gamboa-Herrera JA, Ríos-Reyes CA, Vargas-Fiallo LY (2021) Mercury speciation in mine
523 tailings amended with biochar: Effects on mercury bioavailability, methylation potential and
524 mobility. *Sci Total Environ* 760:143959. <https://doi.org/10.1016/j.scitotenv.2020.143959>
- 525 Ghosh D, Maiti SK (2020) Can biochar reclaim coal mine spoil?. *J Environ Manage* 272:111097.
526 <https://doi.org/10.1016/j.jenvman.2020.111097>
- 527 Głąb T, Gondek K, Mierzwa–Hersztek M (2021) Biological effects of biochar and zeolite used
528 for remediation of soil contaminated with toxic heavy metals. *Sci Rep* 11: 6998.
529 <https://doi.org/10.1038/s41598-021-86446-1>
- 530 Guisquiani PL, Concezzi L, Businelli M, Macchioni A (1998) Fate of pig sludge liquid fraction
531 in calcareous soil: agricultural and environmental implications. *J Environ Qual.* 27:364-371.
532 <https://doi.org/10.2134/jeq1998.00472425002700020017x>
- 533 Guitián F, Carballas T (1976) *Técnicas de análisis de suelos*. Editorial Pico Sacro, Santiago de
534 Compostela.
- 535 Hale SE (2012) Quantifying the total and bioavailable polycyclic aromatic hydrocarbons and
536 dioxins in biochars. *Environ Sci Technol* 46:2830-2838. <https://doi.org/10.1021/es203984k>
- 537 Hartley W, Dickinson NM, Riby P, Lepp NW (2009) Arsenic mobility in brownfield soils
538 amended with green waste compost or biochar and planted with *Miscanthus*. *Environ Pollut* 157:
539 2654-2662. <https://doi.org/10.1016/j.envpol.2009.05.011>
- 540 Hartley W (2010) Arsenic mobility and speciation in a contaminated urban soil are affected by
541 different methods of green waste compost application. *Environ Pollut* 158:3560-3570.
542 <https://doi.org/10.1016/j.envpol.2010.08.015>
- 543 Hendershot WH, Duquette M (1986) A simple barium chloride method for determining cation
544 exchange capacity and exchangeable cations. *Soil Sci Soc Am J* 50:605-608.
545 <https://doi.org/10.2136/sssaj1986.03615995005000030013x>
- 546 Houba VJG, Temminghoff EJM, Gaikhorst GA, Van Vark W (2000) Soil analysis procedures
547 using 0.01 M calcium chloride as extraction reagent. *Commun Soil Sci Plant Anal* 3:1299-1396.
548 <https://doi.org/10.1080/00103620009370514>
- 549 Ippolito JA et al (2015) Biochar elemental composition and factors influencing nutrient retention.
550 In: Lehmann J, Joseph S (eds) *Biochar for environmental management: science and technology*.
551 Earthscan Books Ltd, London, UK, pp139-163
- 552 Kim HB et al (2021) Interaction of biochar stability and abiotic aging: Influences of pyrolysis
553 reaction medium and temperature. *Chem Eng J* 411:128441.
554 <https://doi.org/10.1016/j.cej.2021.128441>
- 555 Kloss S et al (2012) Characterization of slow pyrolysis biochars: Effects of feedstocks and
556 pyrolysis temperature on biochar properties. *J Environ Qual* 41:990-1000.
557 <https://doi.org/10.2134/jeq2011.0070>
- 558 Lehmann J, Joseph S (2015) Biochar for environmental management: an introduction. In:
559 Lehmann J, Joseph S (eds) *Biochar for environmental management*. Routledge, London, UK, pp
560 33-46
- 561 Li G, (2018) Biochars induced modification of dissolved organic matter (DOM) in soil and its
562 impact on mobility and bioaccumulation of arsenic and cadmium. *J Hazard Mater* 348:100-108.
563 <https://doi.org/10.1016/j.jhazmat.2018.01.031>

- 564 Li Z, Ma Z, van der Kuijp TJ, Yuan Z, Huang L (2014) A review of soil heavy metal pollution
565 from mines in China: pollution and health risk assessment. *Sci Total Environ* 468 :843-853.
566 <https://doi.org/10.1016/j.chemosphere.2007.10.022>
- 567 Lin HT, Wang MC, Seshaiiah K (2008) Mobility of adsorbed arsenic in two calcareous soils as
568 influenced by water extract of compost. *Chemosphere*. 71:742-749.
569 <https://doi.org/10.1016/j.chemosphere.2007.10.022>
- 570 Lomaglio T et al (2017) Effect of biochar amendments on the mobility and (bio) availability of
571 As, Sb and Pb in a contaminated mine technosol. *J Geochem Explor* 182:138-148.
572 <https://doi.org/10.1016/j.gexplo.2016.08.007>
- 573 Luo Y (2014) Improvement to maize growth caused by biochars derived from six feedstocks
574 prepared at three different temperatures. *J Integr Agric* 13:533-540.
575 [https://doi.org/10.1016/S2095-3119\(13\)60709-1](https://doi.org/10.1016/S2095-3119(13)60709-1)
- 576 Luo L, Xu CH, Chen Z, Zhang S (2015) Properties of biomass-derived biochars: Combined
577 effects of operating conditions and biomass types. *Bioresour Technol* 192:83-89.
578 <https://doi.org/10.1016/j.biortech.2015.05.054>
- 579 Manyà JJ (2012) Pyrolysis for biochar purposes: a review to establish current knowledge gaps
580 and research needs. *Environ Sci Technol* 46 :7939-7954. <https://doi.org/10.1021/es301029g>
- 581 Mehlich A (1984) Mehlich 3 soil test extractant: A modification of Mehlich 2 extractant.
582 *Commun. Soil Sci Plant Anal* 15:1409-1416. <https://doi.org/10.1080/00103628409367568>
- 583 Mehra OP, Jackson ML (1960) Iron oxide removal from soils and clays by a dithionite-citrate
584 system buffered with sodium bicarbonate. In: Swineford A (ed) *Clays and Clay Minerals*.
585 Pergamon Press, New York, pp 317-327
- 586 Mohan D (2018) Biochar production and applications in soil fertility and carbon sequestration –
587 a sustainable solution to crop-residue burning in India. *RSC Adv* 8:508-520.
588 <https://doi.org/10.1039/C7RA10353K>
- 589 Mombo S et al (2015) Management of human health risk in the context of kitchen gardens
590 polluted by lead and cadmium near a lead recycling company. *J Soils Sediments*. 16:1214-1224.
591 <https://doi.org/10.1007/s11368-015-1069-7>
- 592 Mukherjee A, Zimmerman AR (2013) Organic carbon and nutrient release from a range of
593 laboratory-produced biochars and biochar-soil mixtures. *Geoderma* 193-194:122-130.
594 <https://doi.org/10.1016/j.geoderma.2012.10.002>
- 595 Ouyang W, Zhao X, Tysklind M, Hao F, Wang F (2015) Optimisation of corn straw biochar
596 treatment with catalytic pyrolysis in intensive agricultural area. *Ecol Eng* 84:278-286.
597 <https://doi.org/10.1016/j.ecoleng.2015.09.003>
- 598 Park JH et al (2011) Biochar reduces the bioavailability and phytotoxicity of heavy metals. *Plant*
599 *Soil*. 348:439-451. <https://doi.org/10.1007/s11104-011-0948-y>
- 600 Pérez-Esteban J, Escolástico C, Masaguer A, Moliner A (2012) Effects of sheep and horse manure
601 and pine bark amendments on metal distribution and chemical properties of contaminated mine
602 soils. *Eur J Soil Sci* 63:733-742. <https://doi.org/10.1111/j.1365-2389.2012.01468.x>

- 603 Pietrzykowski M (2019) Tree species selection and reaction to mine soil reconstructed at
604 reforested post-mine sites: Central and eastern European experiences. *Ecol Eng* 3:100012.
605 <https://doi.org/10.1016/j.jenvman.2015.05.036>
- 606 Puga AP, Abreu C, Melo LCA, Beesley L (2015) Biochar application to a contaminated soil
607 reduces the availability and plant uptake of zinc, lead and cadmium. *J Environ Manage* 159:86-
608 93. <https://doi.org/10.1016/j.still.2016.01.008>
- 609 Puga AP et al (2016) Leaching and fractionation of heavy metals in mining soils amended with
610 biochar. *Soil Tillage Res* 164:25-33. <https://doi.org/10.1016/j.still.2016.01.008>
- 611 Rodríguez-Vila A, Forján R, Guedes R.S., Covelo EF (2017) Nutrient phytoavailability in a mine
612 soil amended with technosol and biochar and vegetated with *Brassica juncea*. *J Soils Sediments*
613 17:1653-1661. <https://doi.org/10.1007/s11368-016-1643-7>
- 614 Salbu B, Krekling T (1998) Characterisation of radioactive particles in the environment. *Analyst*
615 123:843-850. <https://doi.org/10.1039/A800314I>
- 616 Sanchez-Monedero MA, Roig A, Martínez-Pardo C, Cegarra J, Paredes C (1996) A microanalysis
617 method for determining total organic carbon in extracts of humic substances. Relationships
618 between total organic carbon and oxidable carbon. *Bioresour Technol* 57:291-295.
619 [https://doi.org/10.1016/S0960-8524\(96\)00078-8](https://doi.org/10.1016/S0960-8524(96)00078-8)
- 620 Shrestha RK, Lal R (2011) Changes in physical and chemical properties of soil after surface
621 mining and reclamation. *Geoderma*. 161:168-176.
622 <https://doi.org/10.1016/j.geoderma.2010.12.015>
- 623 Singh B, Singh BP, Cowie AL (2010) Characterisation and evaluation of biochars for their
624 application as a soil amendment. *Aust J Soil Res* 48:516-525. <https://doi.org/10.1071/SR10058>
- 625 Sizirici B et al (2021) The effect of pyrolysis temperature and feedstock on date palm waste
626 derived biochar to remove single and multi-metals in aqueous solutions. *Sustain Environ Res* 31:
627 1-16. <https://doi.org/10.1186/s42834-021-00083-x>
- 628 Sohi SP, Krull E, Lopez-Capel E, Bol R (2010) A review of biochar and its use and function in
629 soil. *Adv Agron* 105:47-82. [https://doi.org/10.1016/S0065-2113\(10\)05002-9](https://doi.org/10.1016/S0065-2113(10)05002-9)
- 630 Solaiman ZM, Anawar HM (2015) Application of biochars for soil constraints: challenges and
631 solutions. *Pedosphere* 25:631-638. [https://doi.org/10.1016/S1002-0160\(15\)30044-8](https://doi.org/10.1016/S1002-0160(15)30044-8)
- 632 Szufa S (2020) Torrefaction of straw from oats and maize for use as a fuel and additive to organic
633 fertilizers-TGA analysis, kinetics as products for agricultural purposes. *Energies* 13:2064.
634 <https://doi.org/10.3390/en13082064>
- 635 Tack FM (2010) Trace elements: general soil chemistry, principles and processes. In: Hooda PS
636 (ed) *Trace elements in soils*. John Wiley & Sons, Chichester, UK, pp 9-37
- 637 Tessier A, Campbell PG, Bisson M (1979) Sequential extraction procedure for the speciation of
638 particulate trace metals. *Anal Chem*. 51:844-851. <https://doi.org/10.1021/ac50043a017>
- 639 Trippe KM et al (2021) Phytostabilization of acidic mine tailings with biochar, biosolids, lime,
640 and locally-sourced microbial inoculum: Do amendment mixtures influence plant growth, tailing
641 chemistry, and microbial composition? *Appl Soil Ecol* 165:103962.
642 <https://doi.org/10.1016/j.apsoil.2021.103962>

- 643 Uchimiya M, Lima IM, Klasson KT, Wartelle LH (2010) Contaminant immobilization and
644 nutrient release by biochar soil amendment: roles of natural organic matter. *Chemosphere* 80:935-
645 40. <https://doi.org/10.1016/j.chemosphere.2010.05.020>
- 646 Uchimiya M, Ohno T, He Z (2013) Pyrolysis temperature-dependent release of dissolved organic
647 carbon from plant, manure, and biorefinery wastes. *J Anal Appl Pyrol* 104:84-94.
648 <https://doi.org/10.1016/j.jaap.2013.09.003>
- 649 United States Department of Agriculture (USDA) (1982) Soil survey laboratory methods and
650 procedures for collecting soil samples soil survey investigations report n° 1. Washington, U.S.A:
651 U.S. Department of Agriculture.
- 652 Ussiri DA, Lal R (2005) Carbon sequestration in reclaimed mine soils. *Crit Rev Plant Sci* 24:151-
653 165. <https://doi.org/10.1080/07352680591002147>
- 654 Weng L, Temminghoff EJM, Van Riemsdijk WH (2001) Contribution of individual sorbents to
655 the control of heavy metal activity in sandy soil. *Int J Environ Sci Technol* 35 :4436-4443.
656 <https://doi.org/10.1021/es010085j>
- 657 Wu H et al (2017) The interactions of composting and biochar and their implications for soil
658 amendment and pollution remediation: a review. *Crit Rev Biotechnol* 37:754-764.
659 <https://doi.org/10.1080/07388551.2016.1232696>
- 660 Xing J, Xu G, Li G (2021) Comparison of pyrolysis process, various fractions and potential soil
661 applications between sewage sludge-based biochars and lignocellulose-based biochars. *Ecotox*
662 *Environ Safe* 208:111756. <https://doi.org/10.1016/j.ecoenv.2020.111756>
- 663 Xu G, Sun JN, Shao HB, Chang SX (2014) Biochar had effects on phosphorus sorption and
664 desorption in three soils with differing acidity. *Ecol Eng* 62:54-60.
665 <https://doi.org/10.1016/j.ecoleng.2013.10.027>
- 666 Yadav A, Garg VK (2011) Recycling of organic wastes by employing *Eisenia fetida*. *Bioresour*
667 *Technol* 102:2874-2880. <https://doi.org/10.1016/j.biortech.2010.10.083>
- 668 Zhang G et al (2011) Sorption of simazine to corn straw biochars prepared at different pyrolytic
669 temperatures. *Environ Pollut* 159 :2594-2601. <https://doi.org/10.1016/j.envpol.2011.06.012>
- 670 Zhao R, Jiang D, Coles N, Wu J (2015) Effects of biochar on the acidity of a loamy clay soil
671 under different incubation conditions. *J Soils Sediments* 15:1919-1926.
672 <https://doi.org/10.1007/s11368-015-1143-1>
- 673 Zhou L et al (2015) Restoration of rare earth mine areas: organic amendments and
674 phytoremediation. *Environ Sci Pollut Res* 22:7151-17160. <https://doi.org/10.1007/s11356-015-4875-y>
675

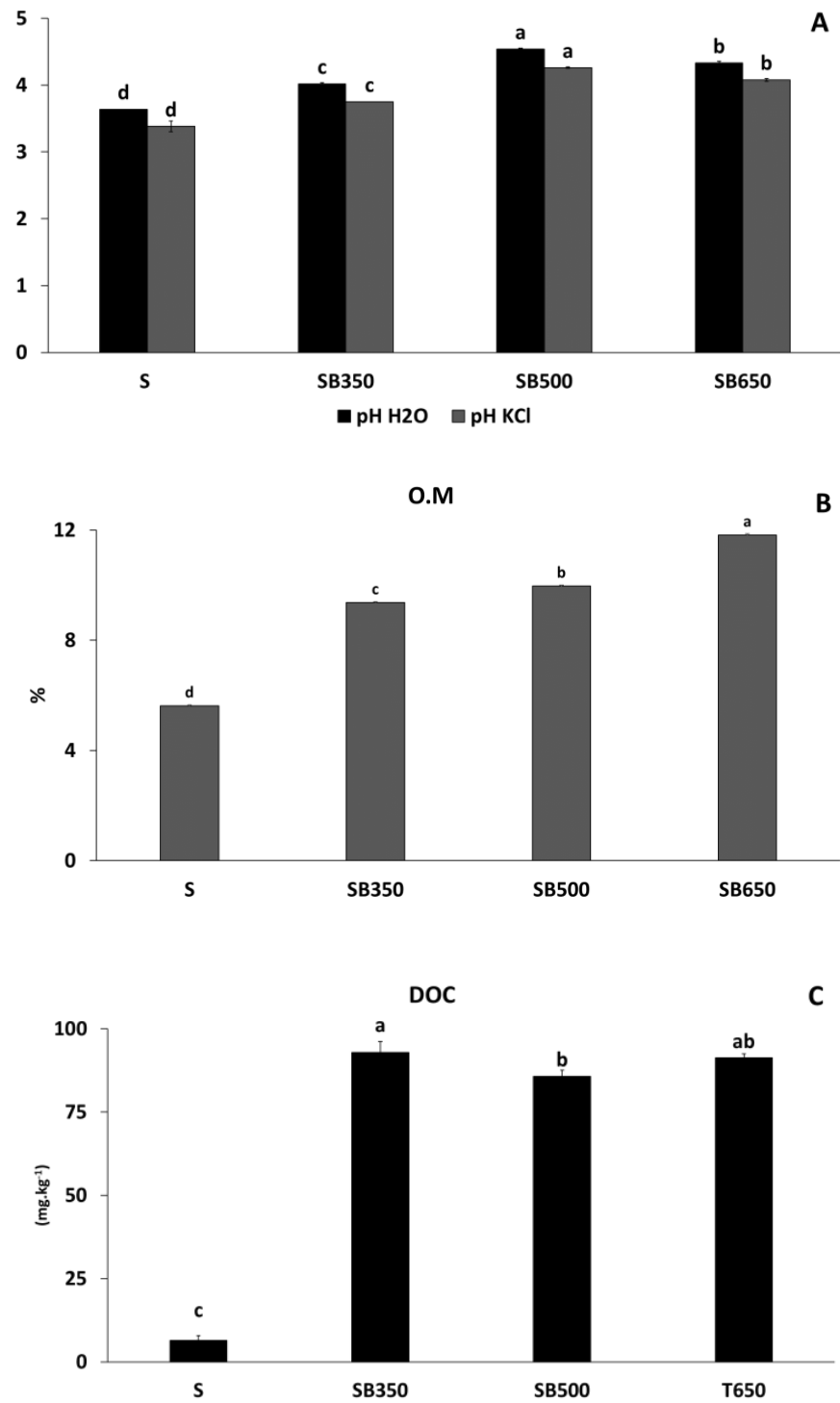


Fig. 1. pH_{H₂O} and pH_{KCl} (A), organic matter (OM) (B), and dissolved organic carbon (DOC) (C) in the control soil and in the different treatments after 40 days.

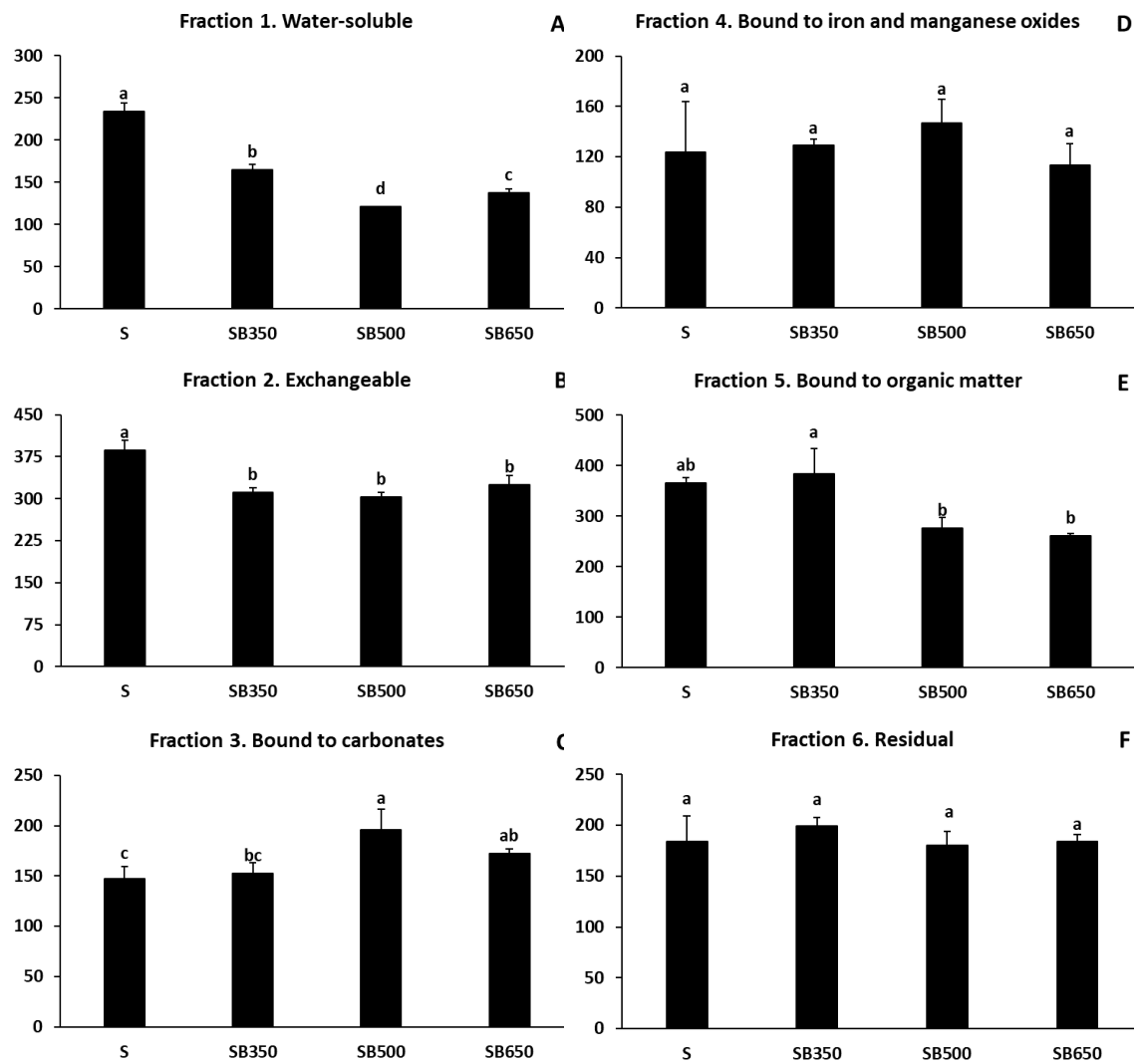


Fig. 2. Evaluation of sequential copper extraction (mg kg⁻¹) where the fractions measured are observed: A (F1), B (F2), C (F3), D (F4), E (F5), F (F6).

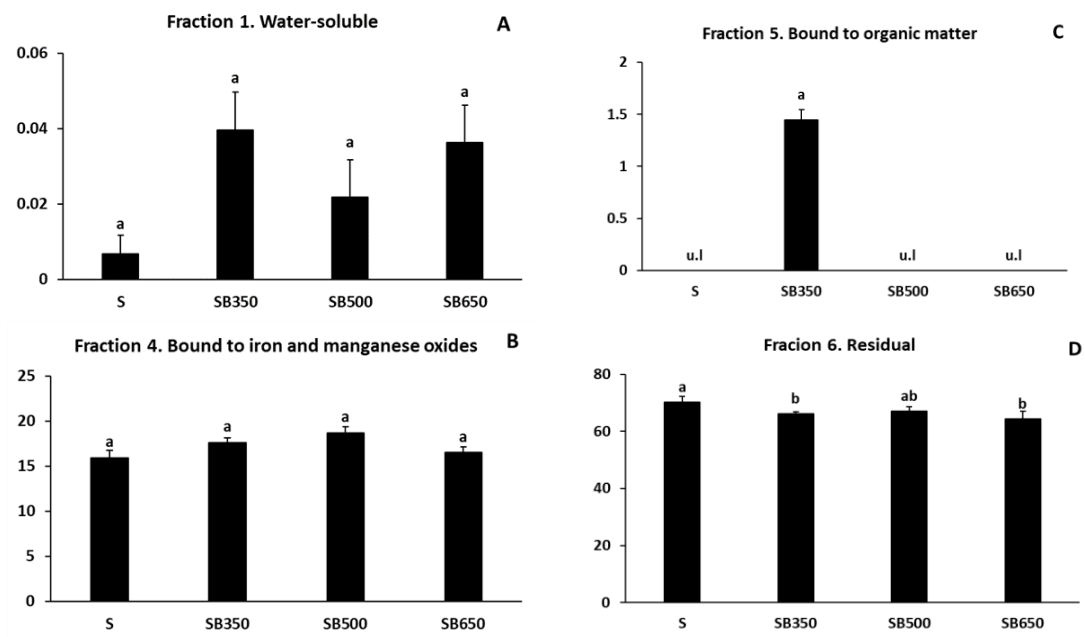


Fig. 3. Concentrations (mg kg⁻¹) of As in F1 (A), F4(B) F5 (C) and F6 (D) from each treatment.

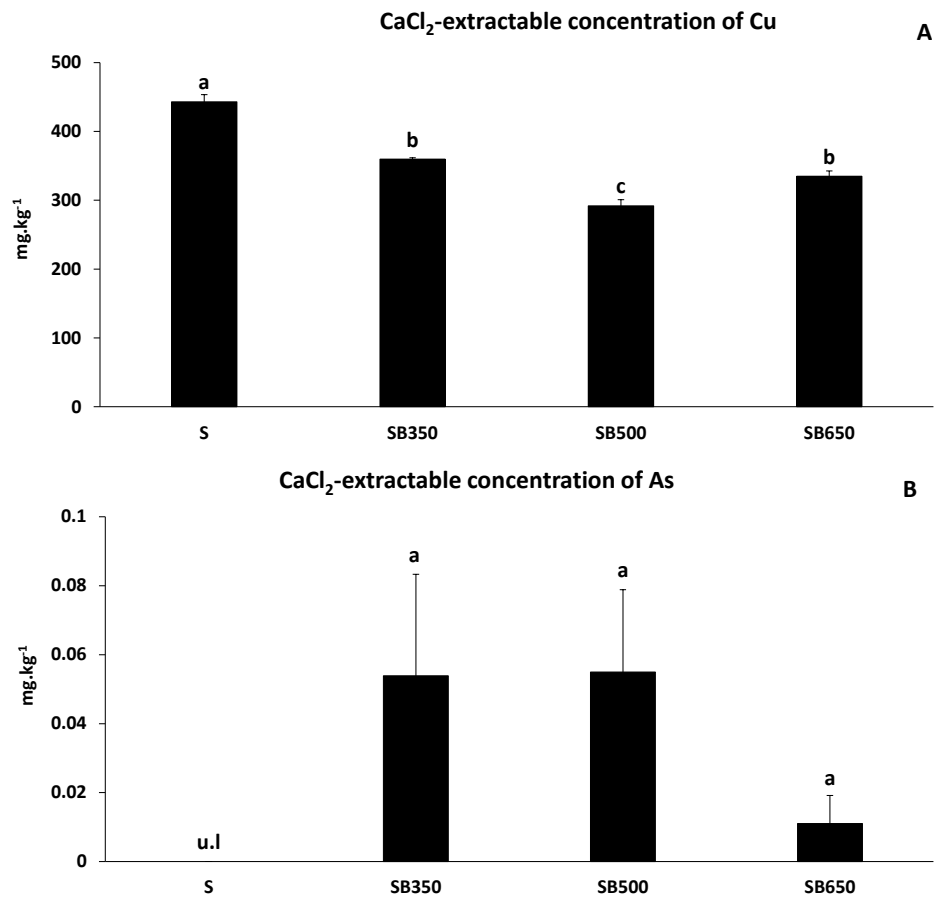


Fig. 4. Graphical representation of CaCl₂ extracted Cu (A) and As (B) after 40-day incubation.

Table 1. Soil and biochar characterization.

Parameter	Units	Polluted Soil (S)	Biochar 350 °C (B350)	Biochar 500 °C (B500)	Biochar 650 °C (B650)
pH H ₂ O	-	3.73 ± 0.01	8.38 ± 0.06	9.95 ± 0.03	10.21 ± 0.02
pH KCl	-	3.49 ± 0.01	7.13 ± 0.01	9.65 ± 0.02	9.91 ± 0.01
SSA D-A	(cm ³ /g)	-	170	346	421
SSA D-R		-	171	347	435
C/H	-	-	0.07	0.11	0.07
C/O	-	-	0.69	1.11	0.74
Sand	%	49.74	-	-	-
Silt		27.45	-	-	-
Clay		22.81	-	-	-
Iron oxides	(mg kg ⁻¹)	3855.65	-	-	-
Aluminum oxides		744.07	-	-	-
Manganese oxides		5.51	-	-	-
OM	%	7.18 ± 0.02	98.18 ± 0.16	96.19 ± 0.15	96.18 ± 0.14
TC	(g kg ⁻¹)	0.15 ± 0.02	72.04 ± 0.07	80.4 ± 0.15	83.01 ± 0.09
DOC		0.05±0.01	0.66±0.02	3.75±0.39	3.67±0.06
TN		0.01 ± 0.00	0.69 ± 0.03	0.67 ± 0.02	0.70 ± 0.01
AP		14.45 ± 0.67	232.78 ± 5.10	120.86 ± 2.46	142.19 ± 3.19
Exchangeable cations	Na ⁺	1.71 ± 0.38	2.10 ± 0.24	3.56 ± 0.89	5.72 ± 0.05
	K ⁺	4.09 ± 0.44	147.24 ± 3.46	378.29 ± 4.57	369.32 ± 6.28
	Ca ²⁺	34.13 ± 0.79	3.97 ± 0.59	2.12 ± 0.27	0.33 ± 0.08
	Mg ²⁺	33.29 ± 0.99	10.88 ± 0.95	1.09 ± 0.13	1.69 ± 0.05
	Al ³⁺	11.60 ± 0.14	< 0.001	< 0.001	< 0.001
	CEC	84.82 ± 0.56	164.20 ± 4.04	385.06 ± 5.22	377.05 ± 6.36
% V	%	86.32	100	100	100
% Al		13.68	u.l.	u.l.	u.l.

Pseudototal	As	85.09 ± 9.94	< 0.001	< 0.001	< 0.001
	Cu	1124.96 ± 10.33	8.50 ± 0.46	4.39 ± 4.06	3.39 ± 5.88

u.l.: undetectable level, BET Surface Area Dubinin- Astakhov (SSA D-A) and Dubinin-Radushkevich (SSA D-R), C/H and C/O ratios, TC: total carbon, TN: total nitrogen, AP: available P, OM: organic matter, DOC: dissolved organic carbon, CEC: cation exchange capacity, %V: base saturation, %Al: aluminium saturation. ±, standard error.

Table 2. Polycyclic aromatic hydrocarbon (PAH) content in the initial soil and the three biochar products.

PAHs ($\mu\text{g}\cdot\text{kg}^{-1}$)		Soil	B350	B500	B650
2-3 ring PAHs	Naphthalene	4	611	3	8
	Acenaphthylene	6	53	3	21
	Acenaphthene	5	92	7	9
	Fluorene	u.l.	117	17	35
	Phenanthrene	24	740	171	480
	Anthracene	3	181	76	128
	Fluoranthene	5	127	87	323
	Pyrene	4	102	79	361
	Benzo[a]anthracene	2	35	49	151
	Chrysene	1	27	35	135
4-6 ring PAHs	Benzo[k]fluoranthene	u.l.	u.l.	22	93
	Benzo[b]fluoranthene	u.l.	u.l.	4	22
	Benzo[a]pyrene	u.l.	u.l.	29	80
	Indeno[1,2,3-c,d]pyrene	u.l.	u.l.	29	49
	Dibenzo[a,h]anthracene	u.l.	u.l.	19	21
	Benzo[g,h,i]perylene	2	u.l.	10	34
Sum 16 PAHs		56	2085	641	1951